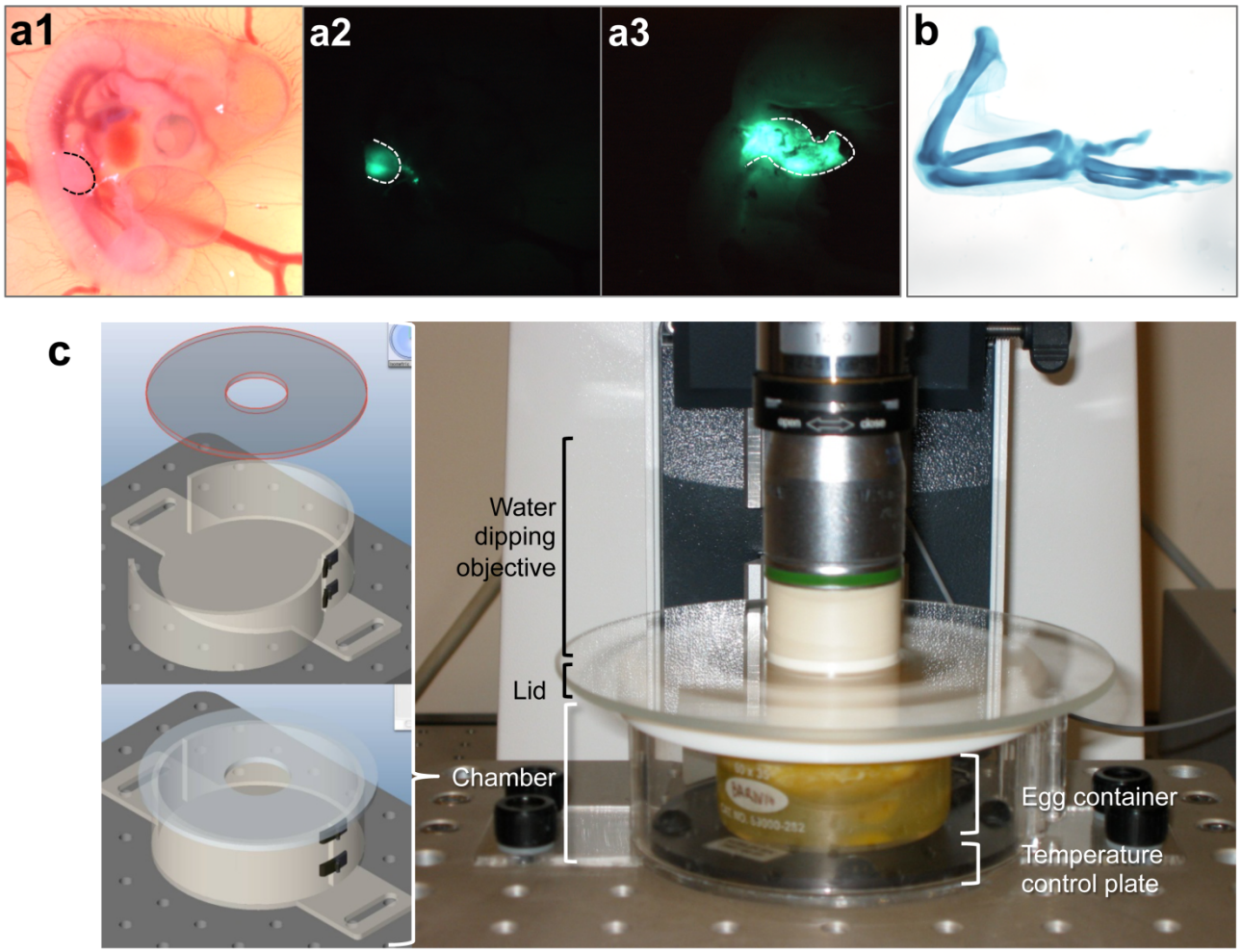

Supplementary Figure 1. Design of a robust system for single cell real-time imaging within living vertebrate embryos. (a) Generating a genetically tractable system in developing chicken embryos with the piggyBac transposable system. Stable integration results in the persistent expression of introduced transgenes. **(a1)** Stage HH 21 chick embryo 48 hours following electroporation of the embryonic coelom visualized *in ovo* demonstrating normal limb bud development. **(a2)** Darkfield image showing pmEGFP expression following piggyBac transposon mediated integration in the right forelimb at 48 hours post electroporation. (**a3)** At E12, 10 days following electroporation, there is maintained pmEGFP expression throughout the limb due to the integration of the piggyBac based expression system. **(b)** Alcian Blue staining demonstrates normal skeletal morphology following electroporation. **(c)** Live *in ovo* microscopy system employs a custom designed environment controlled chamber for maintaining chick embryo development while imaging.

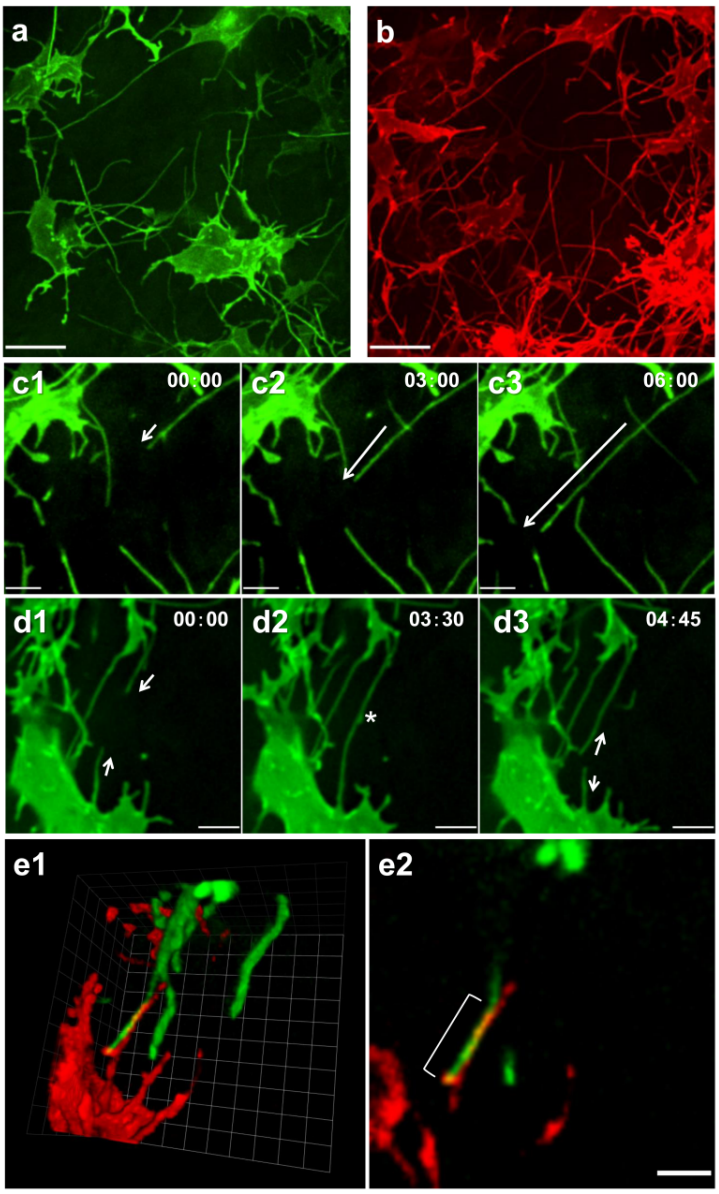

Supplementary Figure 2. Mesenchymal cytoplasmic extensions exhibit complex, dynamic movements and interactions within the three dimensional architecture of the limb bud. (a-b) Individual pmEGFP and pmKate2 channels, respectively, from Figure 1c. Scale = 10µm. **(c1-3)** Timelapse series illustrating the rapid elongation of a representative cytoplasmic extension (see also Supplementary Movie 2). Scale = 5µm. Time min:sec, interval 4 frames/sec. **(d1-3)** Timelapse series showing the interaction between cytoplasmic extensions from different cells that extend toward each other (d1, arrows), interact (d2, asterisk) and then retract (d3, arrows) (see also Supplementary Movie 3). Scale = 5µm. Time in min:sec, interval 4 frames/sec. **(e1)** Three-dimension view illustrating the interaction between cytoplasmic extensions from two distinct cells labeled with the membrane markers pmKate2 and pmEGFP 1 grid unit = 2 µm **(e2)** single confocal plane demonstrating that the two filopodia are in direct contact (see Figure. 1f). Scale = 10 µm.

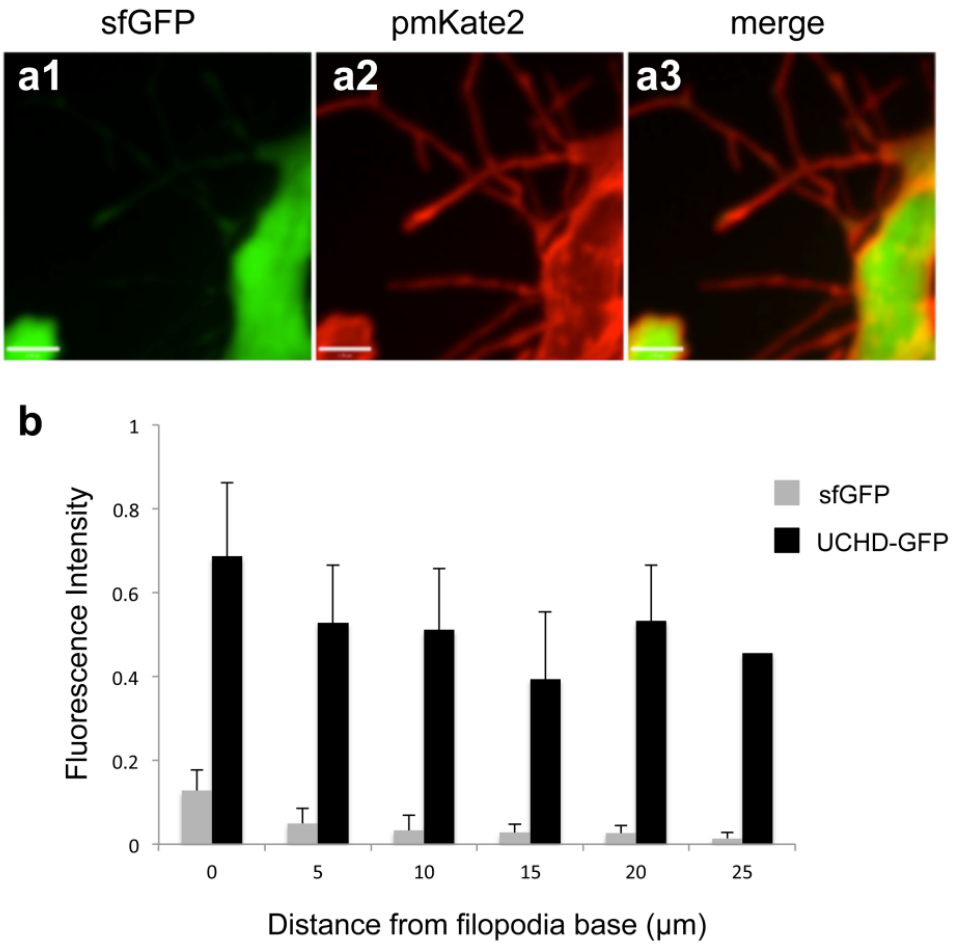

Supplementary Figure 3. Comparative analysis of cytoplasmic fluorescent protein expression and the actin marker UCHD-GFP demonstrates specificity of localization to filopodial extensions. SuperFolder GFP (sfGFP) expression **(a1)** is limited to the cell body when expressed as a cytoplasmic form without an associated targeting sequence and does not extend into filopodia as with the palmitoylated membrane fluorescent protein, pmKate2 **(a2)** merged channels are shown in **a3**. Scale = 3µm **(b)** Normalized fluorescence intensity for sfGFP and UCHD-signals (see Fig. 2a) measured at specific distances along filopodia relative to the cell body (µm) revealing that the UCHD-GFP signal extends far greater distances along filopodial extensions (N=10 filopodia at each measured distance, $p<0.001$).

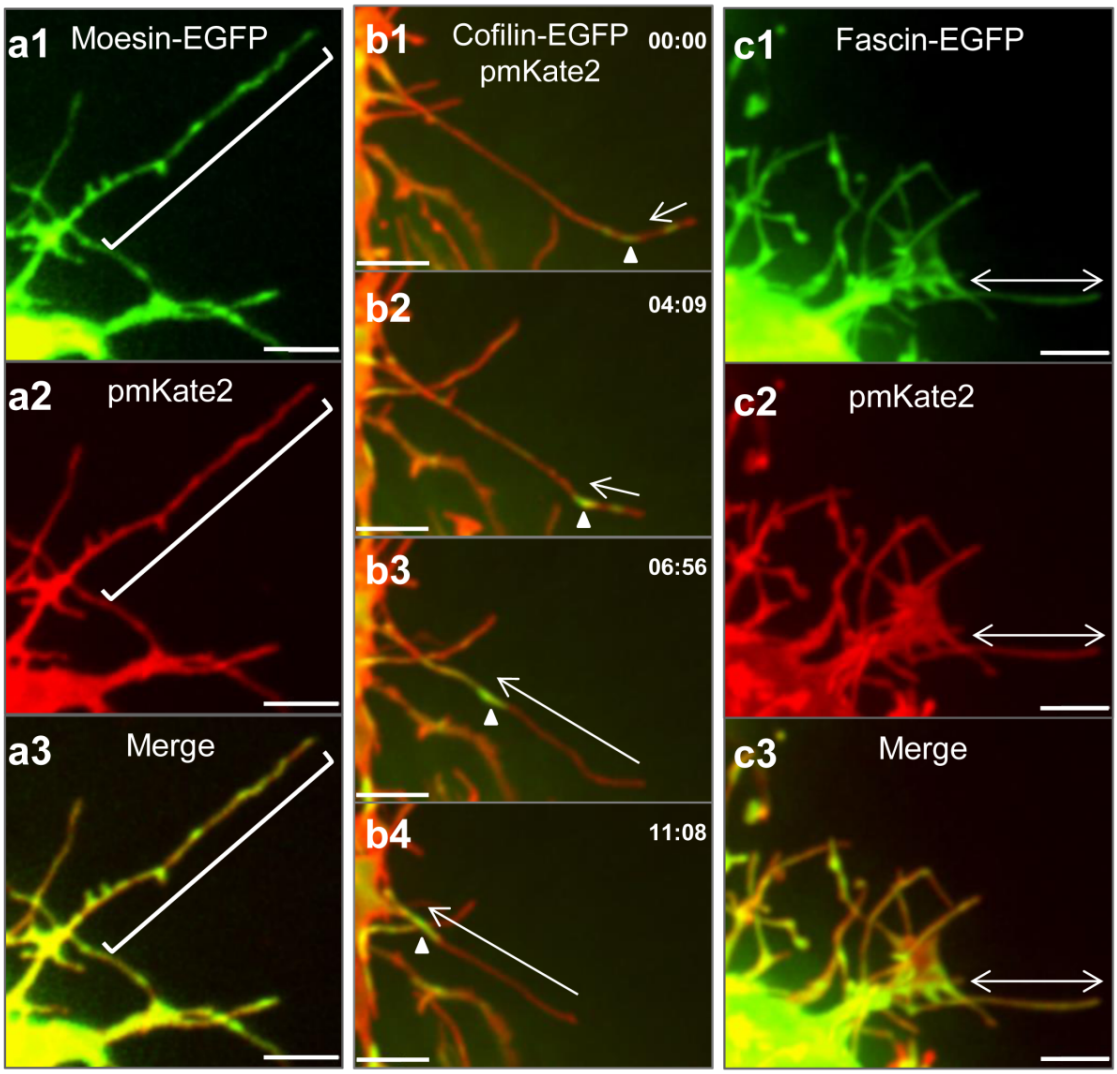

Supplementary Figure 4. Cytoskeleton markers of mesenchymal filopodia (a1-3) The ERM family protein Moesin, is present along the length of filopodia, shown by a bracket, demonstrating an interaction between the cell membrane and the actin skeleton. **(b1-4)** Timelapse imaging revealing the dynamics of Cofilin-EGFP relative to the pmKate2 membrane marker during filopodia retraction. Arrow indicates Cofilin retraction from the filopodia tip to the cell soma (see also Supplementary Movie 6). Time in min:sec. **(c1-3)** Fascin-EGFP uniformly labels filopodia, shown by an arrow. Scale= 5 µm.

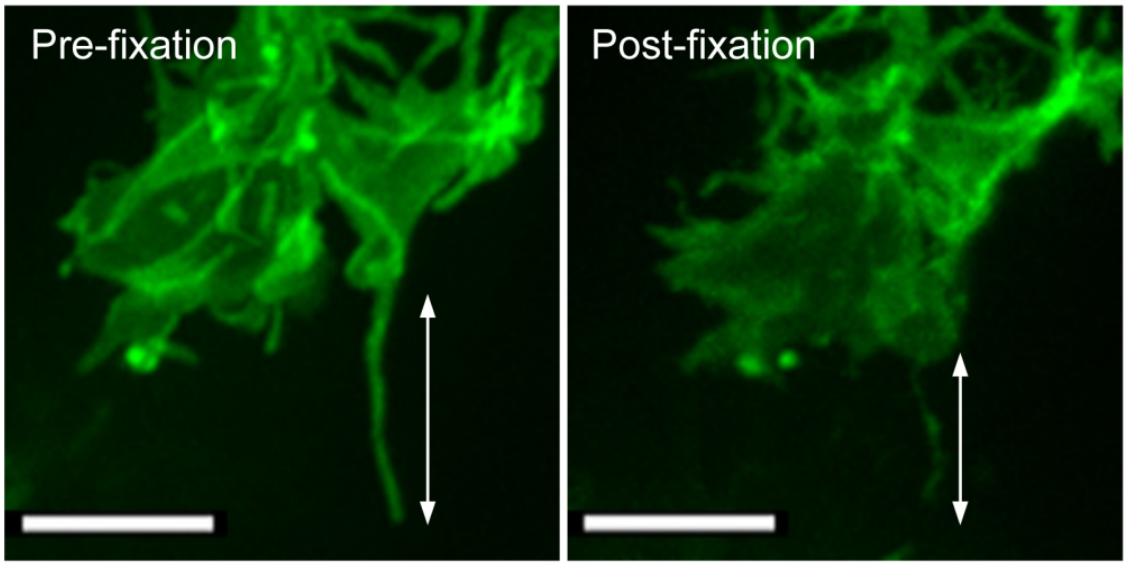

Supplementary Figure 5. Mesenchymal cell filopodia morphology is disrupted following fixation. A limb bud mesenchymal cell prior aldehyde fixation demonstrates typical morphology of filopodia extending from the cell body. This analysis demonstrates that upon fixation, filopodia extensions typically display profound changes to their structure, for example, becoming aberrantly thin and short. In addition, upon fixation there are frequent "breaks" most notably along the distal ends of filopodial extensions. Scale= 10 μm.

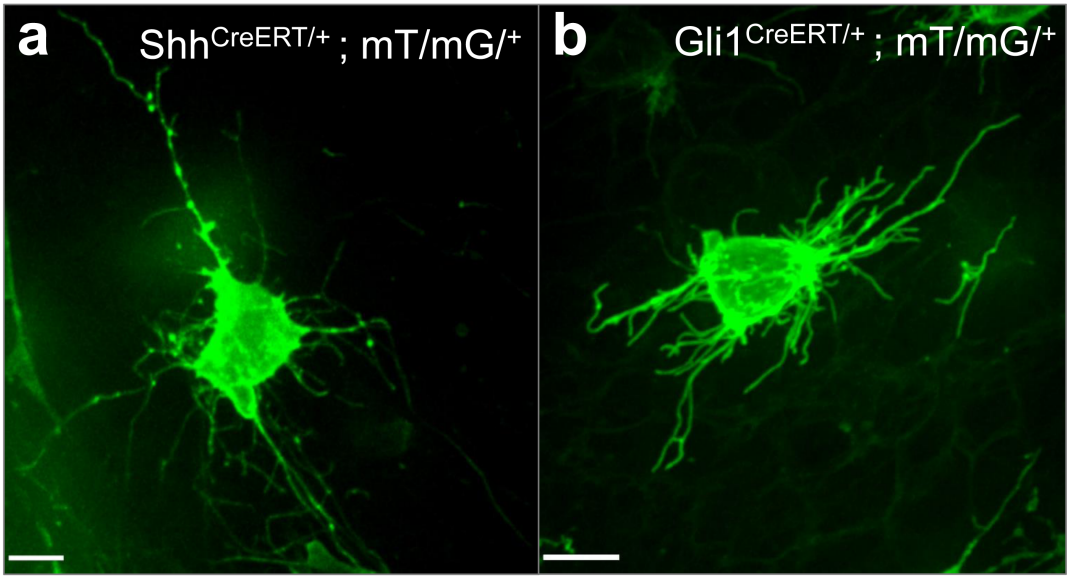

Supplementary Figure 6. Shh producing and responsive cells harbor cytoplasmic extensions within the mouse limb bud. (a-b) The mT/mG transgenic line, a double-florescent Cre reporter mouse, that expresses tandem dimer Tomato (mT) prior to Cre-mediated excision and membrane-targeted enhanced green florescent protein (mG) after excision was employed to mark defined populations of limb mesenchymal cells. (**a**) Shh producing cells within the limb bud of $Shh^{CreERT/+}$; $mT/mG/^{+}$ embryos reveals that they possess multiple long filopodia (see also Supplementary Movie 9) **(b)** Imaging of Shh responding cells within the Shh signaling field of the limb bud within $Gli1^{CreERT/+}$; $mT/mG/^{+}$ embryos reveals that they possess long filopodia similar in appearance to Shh producing cells. Scale= 10 μm

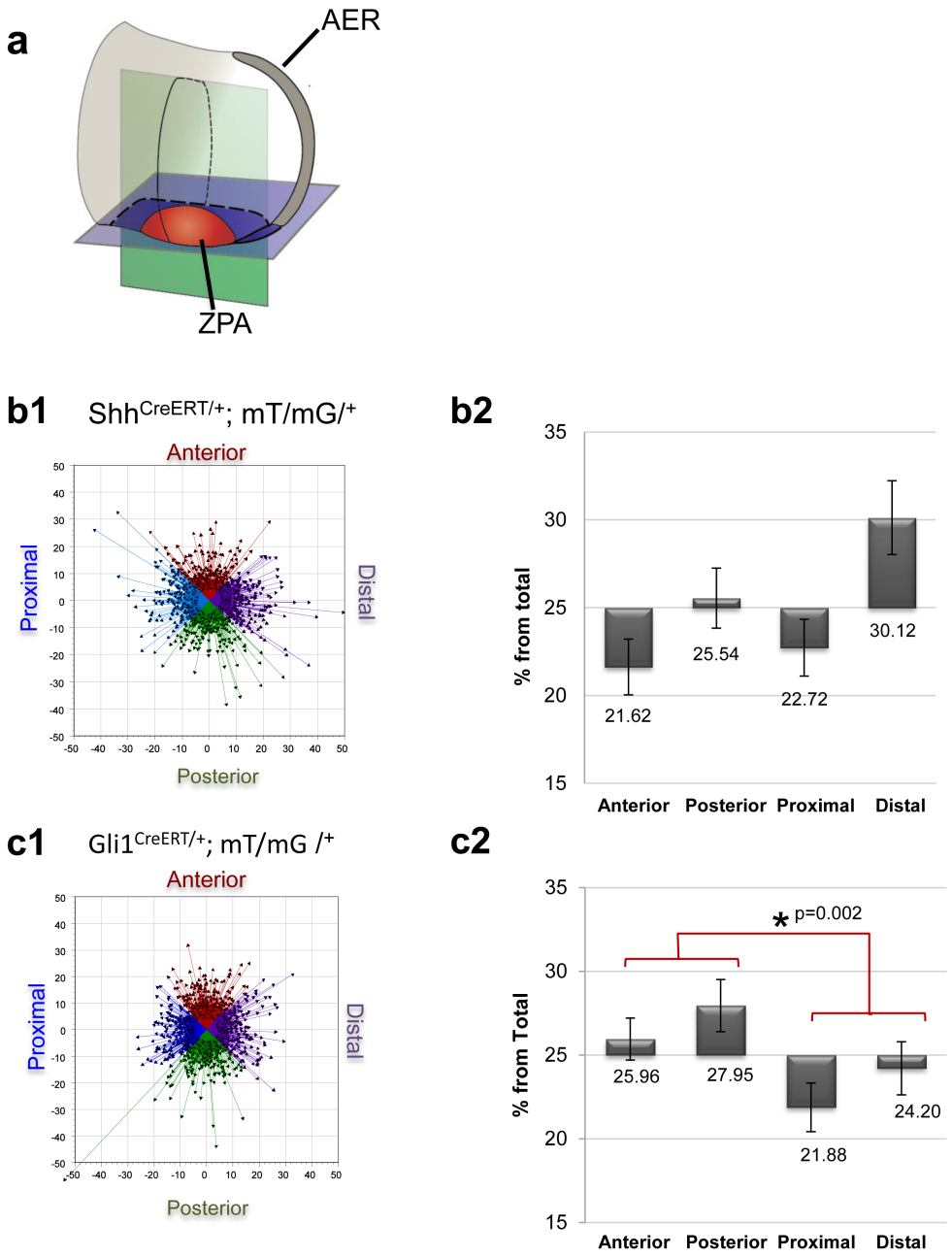

Supplementary Figure 7. Orientation of limb bud mesenchymal filopodia with respect to the Shh signaling axis (a) Schematic illustration of the mouse embryonic limb bud, anterior-top, posterior-bottom, distal-right and proximal-left. The Zone of Polarizing Activity (ZPA) is shown in red the Apical Ectodermal Ridge (AER) in gray. Note that a feedback loop exists between the ZPA and AER. The confocal imaging plane is indicated by the green square. **(b1)** Shh producing mesenchymal cell filopodia orientation was quantified in $Shh^{CreERT/+}$;mT/mG/$^{+}$ embryos and is shown as vectors along the anterior (red) - posterior (green) and proximal (blue) - distal (purple) axes. **(b2)** Analysis of vector orientation by percentage of filopodia orientation along the four limb bud axes. Shh expressing cells can orient along the A-P as well as the Proximal-Distal (Pr-D) axis, with a statistically significant orientation bias towards the distal end of the limb bud where AER resides and maintains the Shh-FGF feedback loop (n=119 cells, 1403 filopodia). **(c1)** Shh responding cell filopodia orientation within the

field of Shh signaling was quantified in Gli1$^{CreERT+/-}$;mT/mG/$^{+}$ embryos and is shown as vectors along the anterior (red) - posterior (green) and proximal (blue) - distal (purple) axes. **(c2)** Analysis of vector orientation by percentage of filopodia oriented along the four limb bud axes. Filopodia present on Shh-responding cells have an orientation bias along the Anterior-Posterior ($p = 0.002$) axis reflecting the axis of Shh signaling along the limb bud (n=110 cells, 1491 filopodia).

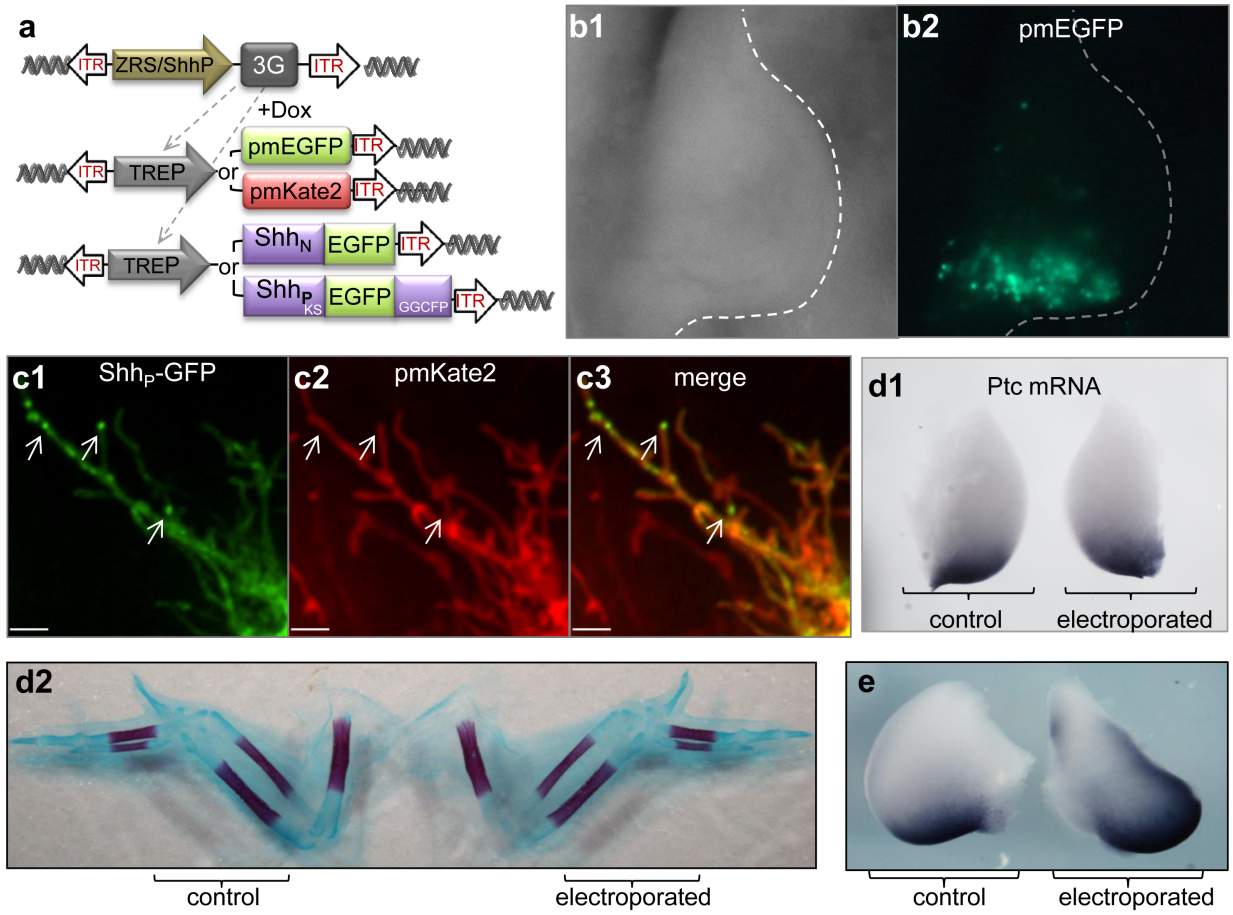

Supplementary Figure 8. Expression of Shh ligand under endogenous regulatory control and activation of Ptc1 expression. (a) Schematic of constructs designed for the expression of specific transgenes in Shh producing cells within the limb bud under native control of the *G. gallus* Shh minimal promoter as well as the zone of polarizing activity regulatory sequence (ZRS) (see Methods). Following the expression of the Doxycycline activator protein (3G), doxycycline (DOX) addition results in the expression of Shh-EGFP forms and a membrane marker from the tetracycline responsive element (TRE). This includes Shh_P-EGFP, where EGFP is inserted into the Shh protein such that both GFP and the cholesterol modification are retained following processing, as well as Shh_N-EGFP, lacking the cholesterol moiety, which produces a brighter and more photostable fluorescent fusion protein. Amino acid residues surrounding the Shh_P-EGFP insertion are shown, KS-EGFP-GGCFP (see Methods). **(b1-2)** Expression of pmEGFP in a stage HH22 forelimb bud following electroporation at stage HH14 with the aforementioned Shh minimal promoter and ZRS regulatory sequence with the addition of DOX control showing a mosaic labeling of cells specifically within the posterior margin of the limb where Shh is normally expressed. **(c1-3)** A representative Shh_P-EGFP positive cell from the limb bud reveals multiple long filopodia with Shh_p-EGFP present in discrete particles as well as more uniform labeling along these extensions also marked with pmKate2. Scale = 5µm. **(d1-d2)** DOX induction of the Shh_N-EGFP molecule under endogenous regulatory control allowed for transient,

mosaic gene expression in a small number of cells within the ZPA, at low levels within the threshold of live cell imaging that does not alter normal Shh signaling as revealed by Ptc1 in situ hybridization nor limb development and skeletal as revealed by alcian blue staining at E12**. (e)** Expression of Shh_N-EGFP from the ubiquitous CAGGS promoter broadly in the limb results in expansion of Ptc1 expression as seen by *in situ* hybridization.

	Particle #	Displacement µm	Displacement stdev	Displacement Normalized	Displacement stdev
Total	38	3.2	5.2	13.4%	35.2
Direction Specific					
Anterograde	23 (61%)	7.1	5.1	29.1%	22.5
Neutral	8 (21%)	-1.2	1.0	-0.1%	2.2
Retrograde	7 (18%)	-3.3	2.8	-14.6%	14.2

Supplementary Figure 9. Shh_N-EGFP particle movement displays net directional anterograde displacement. Net Shh_N-EGFP particle displacement relative to its initial position normalized to filopodia length. Net movement values represented as anterograde positive movement – away from the soma, neutral movement - less than 5% change in overall displacement, and retrograde negative movement – toward the soma. There is a statistically significant difference in net anterograde movement away from the soma toward the tip of the filopodium ($p = 0.0019$). See Figure 3e for graphical representation.

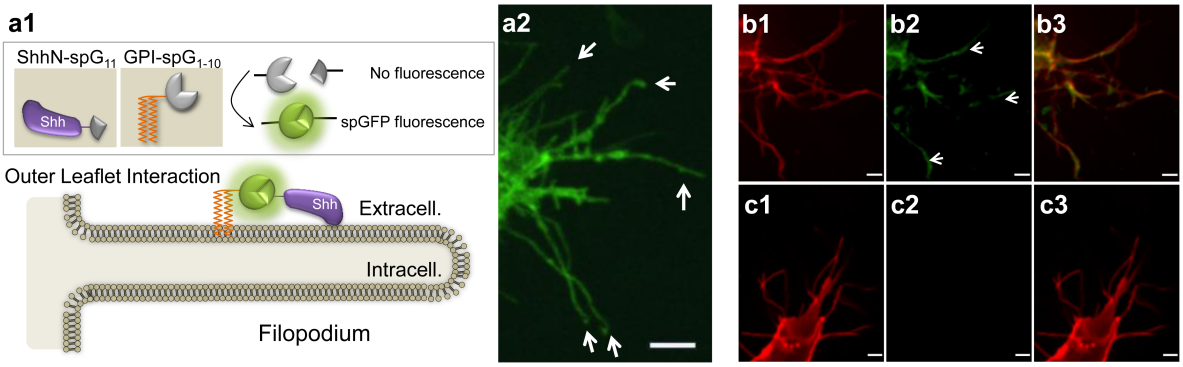

d

In vivo Complementation System

$spGFP_{1-10}$ fusion	$spGFP_{11}$ fusion	GFP Complementation Signal
GPI-$spGFP_{1-10}$	-	-
-	$ShhNspGFP_{11}$	-
GPI-$spGFP_{1-10}$	$ShhNspGFP_{11}$	+

Ex vivo Complementation System

Exogenous $spGFP_{1-10}$ peptide	$spGFP_{11}$ fusion	GFP Complementation Signal
+	-	-
-	$ShhNspGFP_{11}$	-
+	$ShhNspGFP_{11}$	+
-	Cytosolic $spGFP_{11}$	-
+	Cytosolic $spGFP_{11}$	-

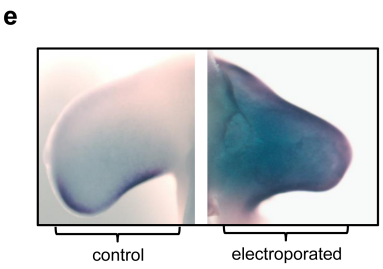

Supplementary Figure 10. **Subcellular localization of Shh_N-EGFP (a1)** Graphical representation of the optimized split GFP complementation system illustrates the spGFP system is comprised of two fragments, $spGFP_{1-10}$ and $spGFP_{11}$, that individually do not form a functional fluorophore however when they associate an irreversible GFP fluorescent signal is produced. **(a2)** Shh_N-$spGFP_{11}$ and an extracellular leaflet membrane associated GPI-$spGFP_{1-10}$ were co-expressed *in vivo*. A positive GFP signal localized to the filopodia membrane (arrows) is observed suggesting that Shh_N is localized to the extracellular surface of the filopodium. **(b1-3)** Limb mesenchyme micromass cultures from a Shh_N-$spGFP_{11}$ electroporated limb bud reveals a complemented GFP signal when the $spGFP_{1-10}$ reagent is added to the culture medium. Arrows reveal areas of GFP intensity along the filopodia membrane. **(c1-3)** Limb mesenchyme micromass cultures from a cytoplasmic localized $spGFP_{11}$ fragment electroporated limb bud upon the addition of the $spGFP_{1-10}$ reagent does not produce any observed GFP signal. pmKate2 serves as a marker of the filopodia membrane. Scale = 3 µm. **(d)** Summary table of the split GFP complementation results for ShhN. **(e)** Shh_N-$spGFP_{11}$ coexpressed with the complementing membrane GPI-$spGFP_{1-10}$ *in vivo* results in ectopic Ptc1 expression as revealed by in situ hybridization.

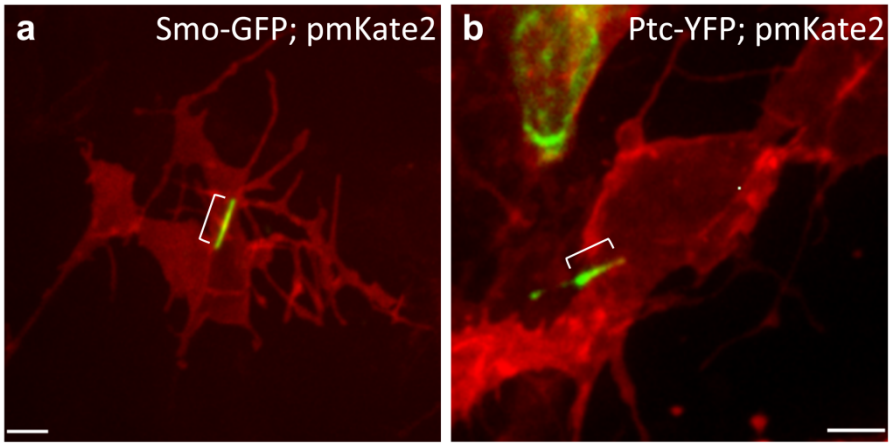

Supplementary Figure 11. Subcellular localization of Smoothened and Patched within mesenchymal cells of the limb bud *in vivo*. (a) Smoothened-GFP is localized to cilia. **(b)** Patched-YFP is dynamically localized in distinct subcellular regions including a perisomal distribution as well as to cilia, in a smaller subset of cells. Scale = 5μm.

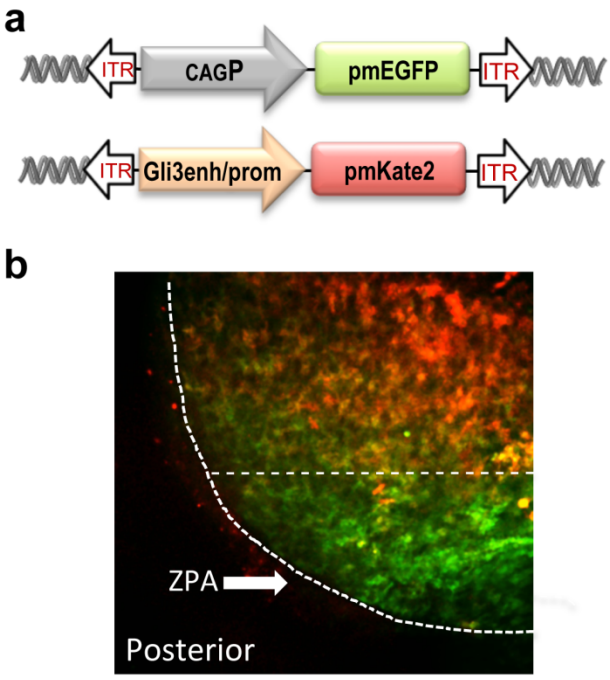

Supplementary Figure 12. Expression system designed to specifically mark the Shh responding cell population of the limb bud. (a) Schematic illustrating the transposon based expression system incorporating the human Gli3 intronic enhancer (hs1586, see Methods) coupled to a minimal rat Gli3 promoter element to express pmKate2 as well as ubiquitous pmEGFP driven by the CAGGS promoter. **(b)** The Gli3 hybrid enhancer/promoter element selectively drives expression of pmKate2 within the limb bud in a region anterior to the ZPA at stage HH21.

Supplementary Methods

Plasmid Expression Constructs

piggyBac transposition system

For extended expression during chicken embryogenesis, the piggyBac transposition system was employed. The parental plasmid pCAG-EBNXN[29] containing the minimal 5'(314 bp) and 3'(242 bp) inverted terminal repeats of the piggyBac transposon[30] was used as the plasmid backbone for expression experiments. PBX contains the CMV enhancer chicken Beta-actin (CAG) promoter expression cassette modified to include the Invitrogen Gateway RfA cassette allowing for phiC31 mediated recombination from Gateway Entry vectors. For doxycycline inducible expression, a modified tetracycline responsive element (TRE)-3G enhancer minimal promoter element (Clontech) replaced the CAG cassette of PBX to generate PBTREX. For the transposase mediated insertion of the piggyBac transposon cassette, the improved piggyBac transposase[31] was expressed via the CAG promoter in the plasmid CAGEN (C. Cepko, Addgene Plasmid 11160[32]). Fluorescent reporter and signaling constructs were introduced into the Gateway system through high fidelity amplification and insertion into pENTR/DTOPO (Invitrogen) as an intermediate to facilitate cloning. The integrity of all constructs was confirmed by DNA sequencing.

Membrane-associated fluorescent proteins

For multicolor labeling of cells and signaling components, the monomeric fluorescent proteins TagBFP (Evrogen), monomeric EGFP (K. Svoboda, Addgene Plasmid 18696[33]), superfolder GFP (sfGFP)[34], mKate2 (Evrogen) as well as oligomeric iRFP (V. Verkhusha, Addgene Plasmid 31857[35]) were selected based on their spectral characteristics as well as their suitability for live imaging of fusion proteins. Inner leaflet membrane-associated palmitoylated fluorescent proteins were generated by the addition of the 20 amino acid sequence of rat GAP-43 MLCCMRRTKQVEKNDEDQKI to the amino terminus of each individual fluorescent protein through sequential PCR amplification, these constructs are designated pm-XFP.

Mosaic expression of membrane fluorescent proteins

For Cre mediated recombination experiments, a loxP–SV40 pA stop–loxP cassette (LSL) (D. Stainier, Addgene 24334[36]) was introduced into the parental ubiquitous and inducible promoter constructs, PB and PB-TRE respectively. pmKate2 and pmEGFP were placed before and after the LSL cassette, respectively, to generate a reporter construct for Cre activity. To generate a self-inactivating Cre

recombinase construct, Cre recombinase containing an amino terminal nuclear localization signal was placed between the lox sites in the PB-LSL vector.

Subcellular Markers

To label F-actin, two markers were employed that show improved cell viability relative to EGFP-actin, Utrophin Ch homodimer-EGFP (D. Mullins) and LifeAct-Kate2. LifeAct-Kate2 was generated by the addition of the 17 aa sequence of Abp140 from *Saccharomyces cerevisiae* and linker sequence MGVADLIKKFESISKEEGDPPVAT to the amino terminus of mKate2 [37,38]. Additional markers of the actin cytoskeleton including bovine Myosin X-heavy meromyosin-EGFP (R. Cheney, [39]), human moesin-EGFP (S. Shaw, Addgene Plasmid 20671[40]), human cofilin-EGFP (J. Bamburg), human fascin-EGFP (D. Vignjevic) were employed. Markers of the tubulin cytoskeleton included Tau-GFP (P. Mombaerts) and EB3-Wasabi (Allele Biosciences). Human Arl13b-mKate2 (J. Reiter) was used as a marker of cilia. Cholesterol modified EGFP was constructed placing amino acids 197-437 of murine Shh on the C-terminal portion of EGFP. The above fluorescent protein constructs were amplified by high fidelity PCR and inserted into pENTR/DTOPO vector and subsequently cloned into piggyBac expression construct.

Shh signaling pathway fusion proteins

Fluorescent fusion proteins were amplified by high fidelity PCR or overlap extension PCR, inserted in the pENTR/DTOPO vector and subsequently cloned into a piggyBac expression construct (see *piggyBac transposition system*). Murine Shh cDNA was provided by Andrew McMahon. Shh_P-EGFP was generated by placing monomeric EGFP between serine196 and glycine197 of murine Shh through overlap extension PCR. We optimized the position of monomeric GFP coding sequence relative to the Shh cholesterol modification site to improve *in vivo* expression[41-43]. This resulted in an improved GFP signal *in vivo*; however, Shh_P-EGFP was less intense than Shh_N-EGFP and other fusion proteins, which may reflect inefficient processing or stability issues[44]. Shh_N-EGFP, a fusion protein lacking the carboxy terminal proteolytic domain and resulting cholesterol addition, was generated by deleting amino acids 197 through 437 following the EGFP fusion. Cdo-GFP and Boc-GFP were made as carboxy terminal fusion proteins[45]. Murine Boc-Kate2 was generated by replacing the cytoplasmic tail GFP with mKate2. Murine Smoothened-TagBFP was generated replacing the fluorophore of Smoothened-GFP (J. Reiter). Patched-YFP (J. Reiter).

spGFP complementation system for Shh

The optimized split GFP complementation system of Cabantous et al. (2004)[46] was employed to assess whether Shh_N-EGFP was localized to the extracellular surface of filopodia. Shh_N-$spGFP_{11}$ was generated by placing the M3 peptide after amino acid 196 of murine Shh separated by a flexible linker, (GGGS)x3. $Shh_N spGFP_{11}$ and the GPI-linked CD14-$spGFP_{1-10}$[47] were inserted into the PB-TRE expression construct. There was no detectable fluorescence observed with either construct independently consistent with previous studies[46].

To further address the subcellular localization of Shh in relation to mesenchymal filopodia, we utilized the exogenous application of a commercially produced $spGFP_{1-10}$ (Sandia Laboratories)[48]. In brief, following the electroporation of the chick embryo somatic lateral plate mesoderm, ex vivo cultures of limb mesenchymal cells were prepared as described in Barna et al. (2007)[49]. Following plating of these cells, the purified $spGFP_{1-10}$ fragment was added exogenously to the live culture and imaged. Positive interaction between the Shh_N-$spGFP_{11}$ and the $spGFP_{1-10}$ was observed as a fluorescent signal 4 hours following reagent addition. As a control for possible endocytosis of the $spGFP_{1-10}$ fragment, a $spGFP_{11}$ luciferase fusion protein localized to the cytoplasm did not produce a fluorescent signal.

G. gallus Shh Promoter and enhancer element:

The 1.7 kb Shh limb specific enhancer element designated the zone of polarizing activity regulatory sequence (ZRS) and 1.1 kb chicken Shh minimal enhancer element[50] were cloned into the PBX vector replacing the CAG promoter cassette to generate a Gateway compatible expression construct. Subsequently, pmEGFP or the tetracycline activator protein 3G (Clontech) were inserted into the expression cassette to allow for either constitutive or doxycycline inducible spatially restricted expression in the ZPA.

Gli3 intronic enhancer and promoter element:

To allow for fluorescent transgenes to be expressed in Shh responding cells of the limb bud, a screen for promoter elements that would correctly regulate expression was performed. In brief, several human enhancer elements identified following ChIP-Seq and mouse transgenic analysis[51] were subsequently tested in chick embryos when coupled to various minimal promoter elements, Hsp68, E1b, thymidine kinase, mimimal CMV. Specific expression was achieved when the human Gli3 intronic enhancer element, hs1586[52] was coupled with the rat minimal Gli3 promoter[53]. Subsequently, pmKate2 (Supplemental Fig. 12) or the tetracycline activator protein 3G (Clontech) were inserted into the

expression cassette to allow for either constitutive or doxycycline inducible spatially restricted expression in the Gli3 expressing and Shh responding cells of the limb.

Chicken Embryo Manipulation and Electroporation

Fertilized chicken eggs (*G. gallus*) were purchased from Petaluma Farms (Petaluma, CA) and subsequently stored at 16°C. Eggs were incubated in a non-rotary incubator at 38.5°C until the desired stage according to Hamburger and Hamilton (HH)[54]. Stage HH13-15 chick embryos were windowed following standard techniques in preparation for electroporation[55]. Embryos were visualized with the assistance of a 470/40 nm bandwidth emission filter, which provided the necessary contrast for injection. PBS without Ca^{2+}/Mg^{2+} was applied to the embryo. The vitelline membrane above the forelimb field was carefully sub-dissected and additional solution was placed over the embryo. DNA constructs, with a final concentration 1- 5µg/µl, diluted in endotoxin free H_2O were combined with Phenol Red (0.1 mM final concentration) to aid in visualization. A 1.0 mm inner diameter capillary glass electrode was backfilled with DNA injection solution and a volume of solution was pressure injected (WPI Picopump) into the embryonic coelom, to completely fill the anterior to posterior extent of the forelimb territory. For the negative electrode, a 250 µm diameter platinum rod with a 4 mm length and 2 mm exposed surface (Nepagene, Japan) was inserted into the yolk and positioned beneath the forelimb field, approximately 0.5-1 mm below the embryo. A 250 µm diameter platinum rod with a 1 mm exposed tip served as the positive electrode and was positioned above the forelimb field with an approximate distance of 2 mm. A square wave pulse train consisting of 8 volts, 3 pulses, 50 ms duration with a 1 sec interpulse interval was delivered via a Nepa 21 electroporator (Nepagene, Japan). This delivery resulted in an approximate current of 8 to 14 mA with energy of 10-18 mJ. Embryos were returned to a 37.5°C for the remainder of the incubation period. In experiments employing the piggyBac transposition system, a 1:5-10 molar ratio of piggyBac transposase helper plasmid, HypBase was combined with the transposon expression construct to mediate integration and high-level expression. This ratio resulted in persistent expression in the embryonic limb through E12, 10 days following electroporation (Supp1ementary Fig. 1a and our unpublished observations). Moreover, limb development and resulting morphology was normal as assessed with Alcian Blue cartilage staining (Supplementary Fig. 1b). For induction of gene expression with the inducible 3G system, 12-24 hours prior to imaging 50 ng doxycycline (Clontech) in 500 µl in Hanks Buffered Saline was injected beneath

the embryonic vasculature. For experiments with iRFP as a fluorescent protein, 75 ng biliverdin (Frontier Scientific) was administered greater than 4 hours prior to imaging.

Live imaging of embryos

To facilitate accessibility of the chick embryo to live imaging with minimal perturbation, embryos were cultured *ex ovo* with improved viability and sustainability[56]. In brief, eggs after 48 hours of incubation at 38.5°C were prepared in sterile fashion and the embryo was directly transferred to a sterile autoclaved 60 mm diameter 35 mm depth crystallization dish by cracking the egg and allowing the albumin and yolk to gently fall into the vessel. Five ml of sterile PBS without Ca^{2+}/Mg^{2+} containing 10x Penicillin/Streptomycin Solution was added to prevent dehydration. The embryo was subsequently covered with a vented sterile lid and placed at 37.5°C. Electroporation was performed as described above. For live imaging on a confocal Axio Examiner system (see confocal microscopy), a custom heated stage top incubator (BioOptechs) was designed allowing for the insertion of a water dipping objective for continuous imaging while maintaining temperature, humidity, and normal growth of chick embryos (Supplementary Fig. 1c).

For imaging with the Zeiss Axio Observer confocal system mouse embryos or electroporated chick embryos were collected into imaging media (DMEM/F12 with HEPES without Phenol Red containing 10% heat inactivated FBS (Invitrogen). Extraembryonic membranes were carefully removed and the entire embryo or the isolated forelimb was transferred and positioned on a 35mm glass bottom culture dish containing a 14 mm German glass coverslip as its base (MatTek Corporation). A 12 mm coverslip was placed above the embryo secured on a ring of Vaseline that served to elevate the coverslip from the embryo, this placement was done to limit the movement of the limb bud during imaging. The chamber containing the embryo or limb bud was placed in a 37°C heated microscope incubator (Solent Scientific) and imaged as described below.

Mice

The mT/mG[57], $Shh^{CreERT2/+}$ [58] and $Gli^{CreERT2/+}$ [59] mice were purchased from Jackson laboratories and maintained on C57BL/6J background. The mT/mG transgenic line is a double-florescent Cre reporter mouse, that expresses tandem dimer Tomato (mT) prior to Cre-mediated excision and membrane-targeted enhanced green florescent protein (mG) after excision to mark defined populations of limb

mesenchymal cells. The mT/mG line is a double-fluorescent Cre reporter line that expresses tandem dimer Tomato (mT) prior to Cre-mediated excision and membrane-targeted enhanced green fluorescent protein (mG) after excision to mark defined populations of limb mesenchymal cells. For induction with tamoxifen, 4 mg of tamoxifen dissolved in corn oil (Sigma) was delivered via orogastric gavage at embryonic day 9.5 and embryonic day 10.5 for $Shh^{CreERT2/+}$; $mT/mG/^{+}$ and $Gli^{CreERT2/+}$; $mT/mG/^{+}$, respectively. For deletion of cdc42 experiments[60], where Cdc42 is critically required for filopodia formation *in vitro*[61], tamoxifen was delivered on E9.5 for $Gli^{CreERT2/+}$; $mT/mG/^{+}$; $cdc42^{loxP/loxP}$. All animals were maintained at The University of California, San Francisco and procedures were performed using IACUC-approved protocols that adhere to the standards of the National Institutes of Health.

Confocal Microscopy

Images were primarily acquired on one of two custom-built spinning disk microscopes. The Zeiss Axio Observer Microscopy system is coupled to a Perkin Elmer UltraVIEW Vox spinning disk confocal microscopy system. The UltraVIEW Vox system utilized 405 nm, 488 nm, 561 nm, and 640 nm solid state laser lines paired with emission filters (Semrock) that were specifically selected to minimize crosstalk across various fluorescent proteins when excited with appropriate solid state sources. Images were captured in the gain mode of a back-thinned electron multiplying CCD camera (Hamamatsu ImageEM C91003). Acquisition of images was accomplished with the Volocity Acquisition suite for multidimensional multichannel time lapse recordings. Laser power and exposure settings were adjusted to minimize photoxicity during the sequence acquisition, power output measured at the entrance to the spinning disk of less than 2.5 mW for all excitation wavelengths.

In ovo imaging was performed on a Zeiss Axio Examiner Microscopy System with a continuous zoom system coupled to a custom built confocal system, with a modified Yokogawa CSU10 scan head that contains an additional patterned array of microlenses. A Hamamatsu ImageEM gain CCD camera was used to capture multichannel and multidimensional images. A custom-built heated stage top incubator allowed for precise insertion of the water-dipping objective for continuous imaging of chick embryos in a micro-controlled environment (Supplementary Fig. 1, see live imaging of embryos).

Image Analysis

Acquired images were processed through the use of the Volocity 6.0 Visualization and Quantification Suites (Perkin Elmer). Image size calibrations were performed for each objective and optivar setting with a calibrated graticule (Electron Microscopy Sciences). Manual measurements of filopodia, fluorescent puncta, and trajectories were obtained across the z space of a three dimensional stack as well as in time for continuous imaging. Volocity recorded values were transferred and processed in Microsoft Excel for subsequent quantification and presentation. For determining filopodia orientation along limb axes, the relative bearing of each filopodial extension across mouse genotypes was categorized into 4 quadrants corresponding to the anterior, distal, posterior and proximal axes. This quadrant categorization, encompassing 45° around the center point allowed for the comparison of vector orientations. Statistical analysis was performed assuming homogeneous distribution of variances and applying Student's t-test between percentages of anterior and posterior orientation versus proximal and distal orientation per cell. For the measurement of fluorescent intensities values, maximal cellular intensity values were obtained with the subsequent subtraction of background fluorescent intensity. Filopodia were manually selected and fluorescent intensity values were determined using Volocity 6.0 Quantification suite. These values were normalized to maximal intensity for the cell to account for differences in protein expression levels. Image presentations were generated in the Volocity 6.0 Visualization suite. For select multicolor confocal acquisitions deconvolution utilizing the calculated point spread function was applied with the Volocity 6.0 Restoration package.

Supplementary References

29. Yusa, K., Rad, R., Takeda, J. & Bradley, A. Generation of transgene-free induced pluripotent mouse stem cells by the piggyBac transposon. *Nat Meth* **6,** 363–369 (2009).
30. Li, X. *et al.* piggyBac internal sequences are necessary for efficient transformation of target genomes. *Insect Mol. Biol.* **14,** 17–30 (2005).
31. Yusa, K., Zhou, L., Li, M. A., Bradley, A. & Craig, N. L. A hyperactive piggyBac transposase for mammalian applications. *Proc Natl Acad Sci USA* **108,** 1531–1536 (2011).
32. Matsuda, T. & Cepko, C. L. Electroporation and RNA interference in the rodent retina in vivo and in vitro. *Proc Natl Acad Sci USA* **101,** 16–22 (2004).
33. Harvey, C. D., Yasuda, R., Zhong, H. & Svoboda, K. The spread of Ras activity triggered by activation of a single dendritic spine. *Science* **321,** 136–140 (2008).
34. Pédelacq, J.-D., Cabantous, S., Tran, T., Terwilliger, T. C. & Waldo, G. S. Engineering and characterization of a superfolder green fluorescent protein. *Nat Biotechnol* **24,** 79–88 (2005).
35. Filonov, G. S. *et al.* Bright and stable near-infrared fluorescent protein for in vivo imaging. *Nat Biotechnol* **29,** 757–761 (2011).
36. Hesselson, D., Anderson, R. M., Beinat, M. & Stainier, D. Y. R. Distinct populations of quiescent and proliferative pancreatic beta-cells identified by HOTcre mediated labeling. *Proc Natl Acad Sci USA* **106,** 14896–14901 (2009).
37. Riedl, J. *et al.* Lifeact mice for studying F-actin dynamics. *Nat Meth* **7,** 168–169 (2010).
38. Riedl, J. *et al.* Lifeact: a versatile marker to visualize F-actin. *Nat Meth* **5,** 605–607 (2008).
39. Bohil, A. B., Robertson, B. W. & Cheney, R. E. Myosin-X is a molecular motor that functions in filopodia formation. *Proc Natl Acad Sci USA* **103,** 12411–12416 (2006).
40. Hao, J.-J. *et al.* Phospholipase C-mediated hydrolysis of PIP2 releases ERM proteins from lymphocyte membrane. *J Cell Biol* **184,** 451–462 (2009).
41. Callejo, A., Quijada, L. & Guerrero, I. Detecting tagged Hedgehog with intracellular and extracellular immunocytochemistry for functional analysis. *Methods Mol Biol* **397,** 91–103 (2007).
42. Vincent, S., Thomas, A., Brasher, B. & Benson, J. D. Targeting of proteins to membranes through hedgehog auto-processing. *Nat Biotechnol* **21,** 936–940 (2003).
43. Vyas, N. *et al.* Nanoscale organization of hedgehog is essential for long-range signaling. *Cell* **133,** 1214–1227 (2008).
44. Chamberlain, C. E., Jeong, J., Guo, C., Allen, B. L. & McMahon, A. P. Notochord-derived Shh concentrates in close association with the apically positioned basal body in neural target cells and forms a dynamic gradient during neural patterning. *Development* **135,** 1097–1106 (2008).
45. Okada, A. *et al.* Boc is a receptor for sonic hedgehog in the guidance of commissural axons. *Nature* **444,** 369–373 (2006).
46. Cabantous, S., Terwilliger, T. C. & Waldo, G. S. Protein tagging and detection with engineered self-assembling fragments of green fluorescent protein. *Nat Biotechnol* **23,** 102–107 (2004).
47. Pinaud, F. & Dahan, M. Targeting and imaging single biomolecules in living cells by complementation-activated light microscopy with split-fluorescent proteins. *Proc Natl Acad Sci USA* **108,** E201–10 (2011).
48. Kaddoum, L., Magdeleine, E., Waldo, G. S., Joly, E. & Cabantous, S. One-step split GFP

staining for sensitive protein detection and localization in mammalian cells. *BioTechniques* **49,** 727–8, 730, 732 passim (2010).
49. Barna, M. & Niswander, L. Visualization of cartilage formation: insight into cellular properties of skeletal progenitors and chondrodysplasia syndromes. *Dev Cell* **12,** 931–941 (2007).
50. Maas, S. A., Suzuki, T. & Fallon, J. F. Identification of spontaneous mutations within the long-range limb-specific Sonic hedgehog enhancer (ZRS) that alter Sonic hedgehog expression in the chicken limb mutants oligozeugodactyly and silkie breed. *Dev Dyn* **240,** 1212–1222 (2011).
51. Visel, A. *et al.* ChIP-seq accurately predicts tissue-specific activity of enhancers. *Nature* **457,** 854–858 (2009).
52. Visel, A., Minovitsky, S., Dubchak, I. & Pennacchio, L. A. VISTA Enhancer Browser--a database of tissue-specific human enhancers. *Nucleic Acids Res* **35,** D88–92 (2007).
53. Cao, D. *et al.* The expression of Gli3, regulated by HOXD13, may play a role in idiopathic congenital talipes equinovarus. *BMC Musculoskelet Disord* **10,** 142 (2009).
54. Hamburger, V. A series of normal stages in the development of the chick embryo. *J Morphol* (1951).
55. Krull, C. E. A primer on using in ovo electroporation to analyze gene function. *Dev Dyn* **229,** 433–439 (2004).
56. Auerbach, R., Kubai, L., Knighton, D. & Folkman, J. A simple procedure for the long-term cultivation of chicken embryos. *Dev Biol* **41,** 391–394 (1974).
57. Muzumdar, M. D., Tasic, B., Miyamichi, K., Li, L. & Luo, L. A global double-fluorescent Cre reporter mouse. *Genesis* **45,** 593–605 (2007).
58. Harfe, B. D. *et al.* Evidence for an expansion-based temporal Shh gradient in specifying vertebrate digit identities. *Cell* **118,** 517–528 (2004).
59. Ahn, S. & Joyner, A. L. Dynamic changes in the response of cells to positive hedgehog signaling during mouse limb patterning. *Cell* **118,** 505–516 (2004).
60. Chen, L. *et al.* Cdc42 deficiency causes Sonic hedgehog-independent holoprosencephaly. *Proc Natl Acad Sci USA* **103,** 16520–16525 (2006).
61. Nobes, C. D. & Hall, A. Rho, rac, and cdc42 GTPases regulate the assembly of multimolecular focal complexes associated with actin stress fibers, lamellipodia, and filopodia. *Cell* **81,** 53–62 (1995).